CrystEngComm

Accepted Manuscript

ROYAL SOCIETY OF CHEMISTRY

www.rsc.org/crystengcomm

ARTICLE TYPE www. rsc.org/xxxxxx | XXXXXXXX

Weak hydrogen and dihydrogen bonds instead of strong N–H···O bonds of tricyclic [1,2,4,5]-tetrazine derivative. Single-crystal X-ray diffraction, theoretical calculations and Hirshfeld surface analysis†

Magdalena Owczarek,*[a,b,c] **Irena Majerz,**[d] **Ryszard Jakubas,**[a]

Received Xth XXXXXXXXXX 20XX, Accepted Xth XXXXXXXXX 20XX
First published on the web Xth XXXXXXXXXX 200X
DOI: 10.1039/b000000x

The octahydro-1H,6H-bis[1,4]oxazino[4,3-b:4',3'-e][1,2,4,5]tetrazine, **1**, and its monohydrated analog, **2**, were obtained in an oxidation process of N-aminomorpholine with iodine. Both compounds crystallize in monoclinic space groups: $P2_1/c$ and $C2/c$ for **1** and **2**, respectively. Despite the presence of a strong hydrogen bond donor – the NH group – crystal packing of **1** is determined by weak C–H···O and C–H···N hydrogen bonds. In order to explore more precisely this intriguing fact, the theory of Atoms In Molecules (AIM) was used to examine intermolecular interactions in a crystal. An analysis of the topological properties of electron density with the determination of bonds critical point revealed a set of contacts which were carefully scrutinized whether they fulfill the criteria of hydrogen and dihydrogen bonds existence in AIM method. Their stability was checked by DFT calculations. In the case of **2**, the crystal packing is realized by strong O1w–H1w···N and N–H···O1w hydrogen bonds with water. The possibility of acceptance more than one hydrogen atom by each lone electron pair of water is discussed on the basis of AIM method and Natural Bond Orbital (NBO) analysis. Hirshfeld surfaces were employed to confirm the existence of intermolecular interactions in **1** and **2**.

1 Introduction

The very first reports on tetrazenes and their tricylic isomers – tetrazines derivatives – appeared in the late 1950s when the existence of a new kind of cation, a diazenium ion, was established[1,2]. The cation was formed during the oxidation process of 1,1-disubstituted hydrazines[3], thermal decomposition of 1,1-disubstituted 2-sulfonylhydrazine salts[4], and in the reaction of secondary amines with difluoroamine[5] or nitrohydroxylamine[6]. Studies showed that the fate of this species strongly depends on the structure of an amine and conditions of a reaction giving in result either nitrogen from the decomposition process, hydrazones as a result of a diazene–hydrazone rearrangement, or tetrazenes[6,7]. To our best knowledge, tricylic aliphatic compounds based on [1,2,4,5]-tetrazine (**i**, see scheme below) were first obtained by the reaction of the Angeli's salt, $Na_2N_2O_3$, with heterocyclic amines, morpholine and piperidine, in the presence of hydrochloric acid[6]. Quite recently, Darwich *et al.*[8] has published the results of kinetic studies of N-aminomorpholine oxidation with chloramine where dipyridododecahydro-s-tetrazine (**i**, X = CH_2) was one of the reaction products. The compound was also formed along with a hydrido iridium(III) phenoxide complex in the reaction of an aminonitrene complex of Ir(III) with phenol[9]. Surprisingly, no structural information of **i** compounds have been available.

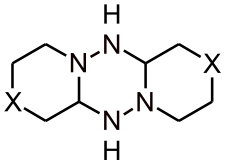

i

X = O or CH_2

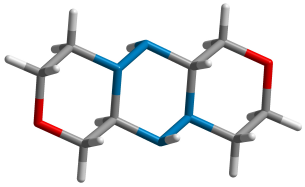

$C_8H_{16}N_4O_2$

Reported herein is an alternative route of a synthesis of octahydro-1H,6H-bis[1,4]oxazino[4,3-b:4',3'-e][1,2,4,5]tetrazine (**i**, X = O; $C_8H_{16}N_4O_2$) and crystal structures of its anhydrous, **1**, and monohydrated, **2**, analogs. Computational methods – Atoms In Molecules theory (AIM) and DFT calculations – allowed to gain insight into the network of intermolecular contacts in **1**. The compound was found to be a perfect example of a substance in which weak

† Electronic Supplementary Information (ESI) available: crystal data and structure refinement parameters. See DOI: 10.1039/b000000x/

[a] *Faculty of Chemistry, University of Wroclaw, F. Joliot Curie 14, 50–383 Wrocław, Poland.*
[b] *Laboratory of Neutron Physics, Joint Institute for Nuclear Research, Joliot-Curie 6, 141–980 Dubna, Russia.*
[c] *Present address: Department of Chemistry, Northwestern University, Evanston, 2145 Sheridan Road, Illinois 60208, USA. E-mail: magdalena.owczarek@northwestern.edu*
[d] *Department of Analytical Chemistry, Faculty of Pharmacy, Wrocław Medical University, Borowska 211a, 50–556 Wrocław, Poland.*

(di)hydrogen bonds are unequivocally responsible for the creation of a crystal, despite the presence of a strong proton donor, the NH group, and an acceptor, the oxygen atom. In the case of **2**, a set of methods (AIM, NBO) was used to address the issue of its unusually high thermal stability, at the same time showing an extraordinary shape of lone electron pairs (LPs) of water oxygen atom. The capability to accept many protons by the water LPs is discussed. Hirshfeld surface analysis concludes the experimental and theoretical results.

2 Results and Discussion

2.1 Synthesis and crystal growth

2 was obtained while performing a synthesis of N-aminomorpholinium iodide. The starting reagents were commercially available N-aminomorpholine (97%, Sigma Aldrich) and hydroiodic acid (57%, Sigma Aldrich) mixed in 1:1 molar ratio in methanol (99.8%, Sigma Aldrich). The mixture was placed in a cooler and after a few days colorless crystals appeared which were identified as **2** using single-crystal X-ray diffraction. On the basis of available information concerning the oxidation process of similar compound – namely, N-aminopiperidine[8] – the possible oxidant in the reaction environment was searched. The most probable seemed I_2 present in hydroiodic acid which was used without previous distillation. Therefore a set of reactions of 4-aminomorpholine with iodine in methanol in the presence of different amounts of water/hydrochloric acid was prepared. Eventually **2** was obtained as follows: 0.04 g I_2 (0.16 mmol) was dissolved in a mixture of 10 mL of methanol, 1 mL of H_2O and 1 mL of HCl. To this solution 2 mL (20.1 mmol) of N-aminomorpholine in 5 mL of methanol was added. The mixture was stored in a cooler ($\sim$4°C) till the appearance of colorless crystals. The process can be schematized by the reactions presented in Scheme 1.

The first step of the process leads to a diazene, **a**, which in the second step, depending on the reaction conditions, gives already structurally characterized 4,4'-bis(morpholine)diazene[10], **b**, or its tricyclic isomer, **c**, which is known to form over **b** in protic media[6]. Single crystals of **1** were obtained by reducing the amount of water and by very slow evaporation at constant temperature ($\sim$4°C).

2.2 Thermal properties

Thermogravimetric analysis (TGA) of **1** showed one distinct weight loss process ($\sim$5%) starting at 330 K which is reflected on the DTA curve as a wide endothermic peak (Fig. 1a). An irreversible heat anomaly with an entropy effect of 16 ± 2 J/molK was also disclosed by the DSC method in a heating cycle (Fig.1a, inset). The origin of this thermal instability is discussed further in the text. Above 400 K the compound melts and gradually decomposes. **2** is thermally stable up to 415 K (Fig.1b). Above this temperature the compound loses 3% of its mass which is ascribed to partial dehydration. A sharp endothermal peak at DTA at *ca.* 480 K is due to a melting process of the sample. A decomposition process starts above 540 K.

DSC measurements of **1** and **2** did not disclose any phase transitions in the temperature range between 100 and 300 K.

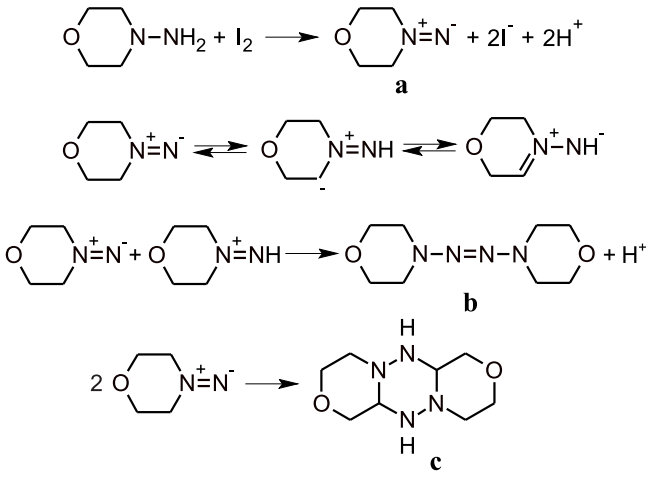

Scheme 1 Formation of 4,4'-bis(morpholine)diazene, **b**, and its tricyclic isomer, **c**, from N-aminomorpholine.

2.3 Structural characterization

The single-crystal X-ray diffraction studies at 100 K revealed that **1** adopts the monoclinic space group $P2_1/c$ (see Table 1). Fig. 2a shows the crystal packing as seen in the [010] direction. The molecules lie on crystallographic inversion centers and are connected into chains *via* weak C1–H1B$\cdots$O1 hydrogen bonds. Three-dimensional packing is realized by linking the chains by intermolecular C4–H4A$\cdots$N1 interactions (Fig. 2b). Geometrical parameters of these hydrogen bonds are collected in Table 2. Weaker hydrogen and dihydrogen bonds were disclosed and analyzed with theoretical methods.

The hydrated analog, **2**, crystallizes in the monoclinic space group $C2/c$. Again, the organic molecules are located on crystallographic inversion centers. The O1w atom of water molecule occupies a special position on a 2-fold rotation axis. The crystal structure of **2** is characterized by the presence of layers (Fig. 3) which formation is possible due to the donor/acceptor properties of water. Each H_2O molecule is a donor of two hydrogen bonds of O–H$\cdots$N type and an acceptor of two hydrogen bonds of N–H$\cdots$O type (Table 2).

	1	**2**
Empirical formula	$C_8H_{16}N_4O_2$	$C_8H_{18}N_4O_3$
Formula weight ($g{\cdot}mol^{-1}$)	200.25	218.26
Temperature (K)	100(2)	100(2)
Wavelength (Å)	0.71073	0.71073
Crystal system, space group	Monoclinic, $P2_1/c$	Monoclinic, $C2/c$
a (Å)	9.789(5)	19.088(5)
b (Å)	6.441(3)	4.672(3)
c (Å)	7.862(4)	12.691(5)
β (°)	112.18(5)	115.56(3)
V (Å^3)	459.0(4)	1021.0(8)
Z	2	4
D_{calc} ($Mg{\cdot}m^{-3}$)	1.449	1.420
μ (mm^{-1})	0.11	0.109
Measured reflections	3621	8486
Independent reflections	1349	2375
Observed reflections $[I > 2\sigma(I)]$	1159	1970
R_{int}	0.015	0.021
Data/restraints/parameters	1349/0/64	2375/0/72
Goodness-of-fit on F^2	1.13	1.07
Final R indices$[I > 2\sigma(I)]$	R_1 = 0.0434	R_1 = 0.0372
	wR_2 = 0.1300	wR_2 = 0.1083
R indices (all data)	R_1 = 0.0478	R_1 = 0.0432
	wR_2 = 0.1333	wR_2 = 0.1116
Weighting parameter a/b	0.0848/0.054	0.0707/0.1903
$\Delta\rho_{max}/\Delta\rho_{min}$ ($e{\cdot}Å^{-3}$)	0.46/-0.27	0.50/-0.26

$w = 1/[\sigma^2(F_0^2) + (aP)^2 + bP]$ where $P = (F_0^2 + 2F_c^2)/3$

Table 1 Selected crystal data and structure refinement parameters of **1** and **2** at 100 K

D–H···*A*	*D*–H	H···*A*	*D*···*A*	∠(*D*H*A*)
1				
C1–H1B···O1^{i}	0.99	2.64	3.463(3)	141
C4–H4A···N1^{ii}	0.99	2.62	3.5646(18)	160
2				
N2–HN2···O1w^{iii}	0.91	2.32	3.1924(15)	161
O1w–H1w···N2	0.86	2.04	2.8851(13)	168

Symmetry codes: (*i*) -*x*+1, -*y*+1, -*z*-1; (*ii*) -*x*+2, *y*-1/2, -*z*+1/2; (*iii*) *x*, *y*+1, *z*.

Table 2 The hydrogen bonds parameters (Å, °) of **1** and **2** at 100 K

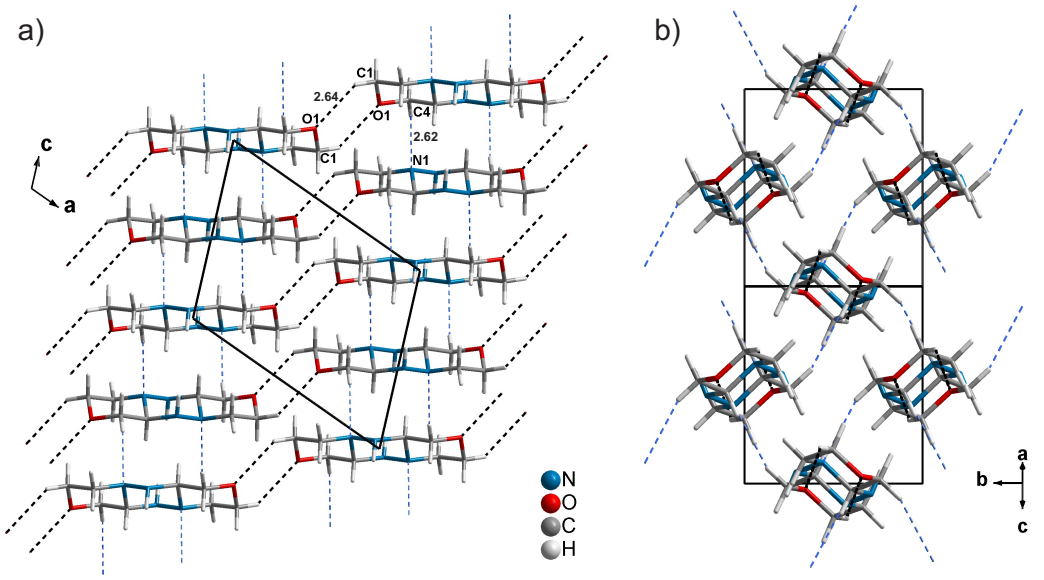

Fig. 2 a) The projection of the structure of **1** along [010]. b) Three-dimensional network formed by C–H···O/N hydrogen bonds. The values of H···A distance of hydrogen bonds are given.

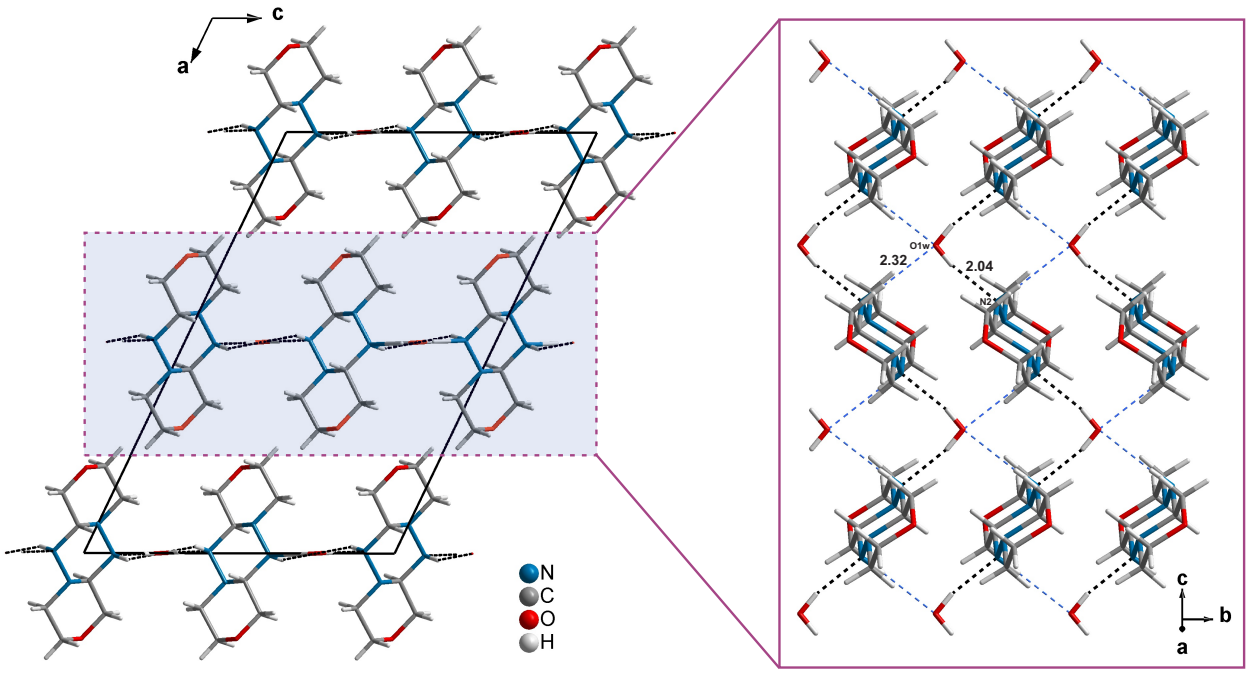

Fig. 3 Crystal packing of **2** along the [010] direction (left part) and the projection of the layer (right part). The values of H···A distance of hydrogen bonds are given.

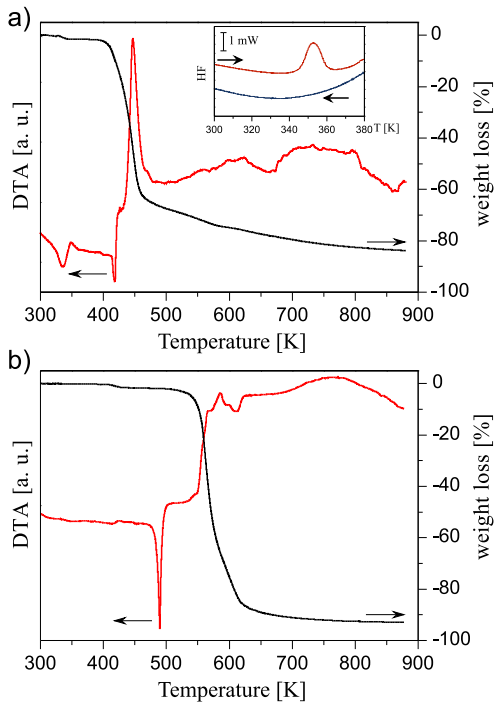

Fig. 1 Simultaneous thermogravimetric and differential thermal analyses scan (ramp rate: 2 K/min) obtained for **1** (a) and **2** (b). Inset in a): DSC curves of **1** for heating and cooling runs (5 K/min, m = 6.772 mg).

2.4 Computational results

The most important rule determining the packing of molecules in crystal says that the hydrogen from strong proton donor group must be engaged in a hydrogen bond which determines the mutual orientation of the molecules linked by a hydrogen bond [11]. The NH group and oxygen atom in $C_8H_{16}N_4O_2$ molecule suggest that the main interaction responsible for the packing of molecules in the crystal should be the N–H···O hydrogen bond. In order to check whether there are any steric hindrances preventing molecules from forming such a bond, and to explain the observed parallel arrangement of molecules in the crystal structure of **1**, we performed optimization of a structural motif in which one molecule, m_1, is approaching second molecule, m_2, with its oxygen atom pointed directly towards the NH group of m_2 (Fig. 4). Such an arrangement is stable as long as m_1 is rotated by about 90 degrees, relative to the donor. Calculated energy of this perpendicular arrangement is *ca.* 0.55 kcal/mol lower than one obtained for two molecules aligned parallel. What is more, m_1 and m_2 molecules are linked by a highly linear N–H···O hydrogen bond which parameters are given in Fig. 4. Therefore, an obvious question: why the parallel arrangement of molecules, where only weak hydrogen bonds can be found and which is also energetically less stable, is still more favorable in the crystal? The question is not a trivial one. It seems that in the case of $C_8H_{16}N_4O_2$ molecules the Kitaigorodskii's principle of the closest packing [12] plays a crucial role in the building of a crystal. However, there are known examples of crystal structures with a non-planar arrangement of a molecules where the principle of the closest packing is realized by a 'herring bone' arrangement which should be the most appropriate for $C_8H_{16}N_4O_2$ as well. And since the values of energy given above strongly convince that a structure with molecules organized in a fashion shown in Fig. 4 can and should exist, it is likely enough that the crystal structure of **1** is only one of the possible polymorphic form of $C_8H_{16}N_4O_2$.

The analysis of the geometry of molecules in the crystal suggests that the strongest interactions responsible for the packing of the molecules in the crystal lattice of **1** are the C–H···O and C–H···N hydrogen bonds. Anyway, more precise analysis performed with AIM theory [13–15] shows more complex set of the molecular interactions listed in Table 3 and shown in Fig. 5.

The value of electron density at the bond critical point (BCP) can be used as a measure of strength of the interactions more precisely than the geometrical parameters [16–19]. According to the electron density values at BCP the strongest hydrogen bond in the investigated crystal (**1**) is the C4–H4A···N1 hydrogen bond parallel to the *c*-axis. Except this hydrogen bond the $C_8H_{16}N_4O_2$ molecules of **1** are linked with identical molecules located along the *c*-axis with a set of very weak and

not very common interaction (see Fig. 5a) listed in Table 3. The first one is another HB of C–H···N type, C3–H3···N2, with twice smaller electron density than the strongest C4–H4A···N1. Along this direction, the oxygen atom is an acceptor of two protons in weak C–H···O hydrogen bonds. Additionally, CH and NH groups are engaged in dihydrogen bonds. Two identical C–H···O hydrogen bonds form a cyclic dimer linking two $C_8H_{16}N_4O_2$ molecules (Fig. 5b). The electron density value of 0.0068 a.u. as well as the H···O distance of 2.640 Å confirms a typical, moderately strong C–H···O hydrogen bond.

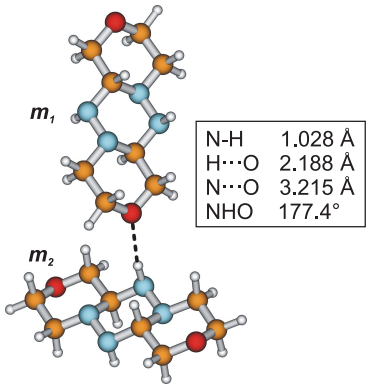

Fig. 4 An optimized perpendicular arrangement of $C_8H_{16}N_4O_2$ molecules and geometrical parameters of NHO hydrogen bond.

The first step of analysis of very weak interactions should be confirmation that these interactions really exist and the best method to do this is checking if an interaction fulfills the criteria of hydrogen bond existence in AIM method[20–22]. The values of the electron density, the Laplacian of electron density at the BCP (criteria range: 0.002–0.035 a.u. and 0.024–0.139 a.u. for $\rho(r)$ and $\nabla^2\rho(r)$, respectively) as well as the shape of the bond paths linking the proton and acceptor atom confirm the existence of every hydrogen bond shown in Fig. 5. The contours of the electron density for particular hydrogen bonds (in the *c* direction) in **1** are shown in Fig. 6. The C–H···N hydrogen bond is the strongest and seems to be responsible for the dimer formation. Similarly, the C–H···O hydrogen bonds are rather typical including the C–H···O formed by common acceptor, but the existence of N–H···H–C and C–H···H–C interactions is usually not evident and therefore their parameters were compared with other dihydrogen bonds known so far. Their geometry is typical for H···H interactions[23] and the electron density, Laplacian and energies at the bond critical points are characterized by similar values[24,25]. Among the weak interactions in the investigated crystal, these dihydrogen bonds are one of the weakest. Despite similarity of the electron density, both dihydrogen bonds are different in regards to the charge value at the hydrogen atoms. According to general classification of dihydrogen bonds[26,27] more pop-

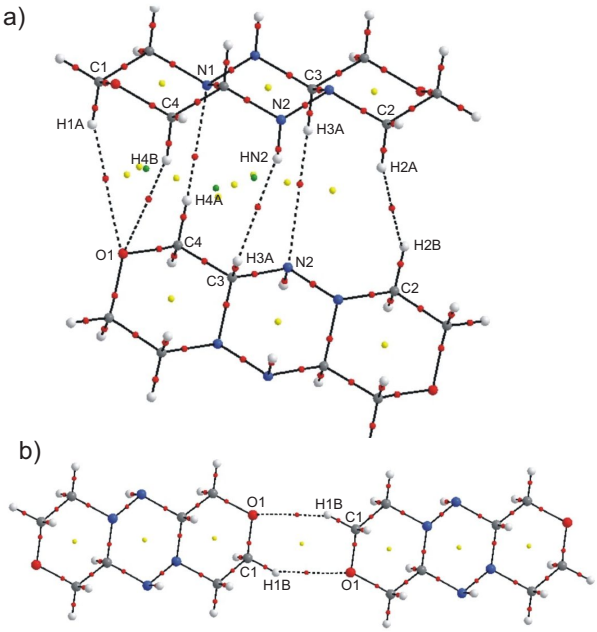

Fig. 5 a) Hydrogen bonds linking the molecules along the *c*-axis. b) C–H···O hydrogen bonds link the $C_8H_{16}N_4O_2$ molecules of **1** perpendicular to the *a*-axis. Small circles are attributed to critical points: red, bond critical point; yellow, ring critical point; green, cage critical point.

Bond	H···A (Å)	ρ(r)	$\nabla^2\rho$(r)	G(r)	V(r)	H(r)	ε	d
C4–H4A···N1	2.618	0.0100	0.0264	0.6946	-0.6634	0.0312	0.0125	0.0030
C3–H3···N2	3.003	0.0047	0.0136	0.3259	-0.2668	0.0591	0.0436	0.0035
C4–H4B···O1	2.806	0.0039	0.0150	0.3274	-0.2246	0.1028	0.1501	0.0118
C1–H1A···O1	2.876	0.0050	0.0178	0.4009	-0.2948	0.1060	0.0585	0.0118
N2–HN2···H3–C3	2.412 (H···H)	0.0040	0.0160	0.3427	-0.2246	0.1181	0.2124	0.0551
C2–H2A···H2B–C2	2.440 (H···H)	0.0042	0.0157	0.3442	-0.2387	0.1056	0.1932	0.0334
C1–H1B···O1	2.636	0.0068	0.0242	0.5753	-0.4703	0.1049	0.0581	0.0123

[a] ρ(r), the electron density; $\nabla^2\rho$(r), the Laplacian of the electron density; G(r), the electron kinetic energy density [a.u.]; V(r), the electron potential energy density [a.u.]; H(r), the electron energy density [a.u.]; ε, the ellipticity; d, the deviation from linearity [Å].

Table 3 The characteristic of the bond critical point (BCP) of the intermolecular hydrogen bonds in **1**[a]

ular are these with similar charges at the H atoms called van der Waals dihydrogen bonds than normal dihydrogen bonds with significant differentiation of the charge at H···H atoms. In the case of the dihydrogen bonds in **1**, the C–H···H–C belongs to the van der Waals interaction with the charges in the proton atomic basin of -0.061 and -0.1030 (Muliken charges of 0.1213, 0.1115). The C–H···H–N is a typical dihydrogen bonds with the charges equal 0.3841 (HN) and -0.1849 (CH) (Muliken charges 0.2535 and 0.0823 respectively).

AIM parameters listed in Table 3 can be very useful in comparison of the strength and stability of the hydrogen bonds[28–35]. As mentioned above, the strongest interactions are connected with the highest values of the electron density at BCP. The Laplacian of the electron density is a basis for a general classification of the interatomic interaction which can be divided into two general classes: *shared interactions* where the electric charge is concentrated between two nuclei (negative values of $\nabla^2\rho$(r)), and *closed-shell interactions* characterized by depletion of the charge in the interatomic space and concentration towards each of the interacting nuclei. Hydrogen bonds and van der Waals' complexes belong to the closed-shell type. Covalent and polar bonds represent the shared interaction.

When the electron density at BCP characterizes the strength of the interaction and the Laplacian of electron density at BCP can be used as classification of the interaction, other parameters as ellipticity and energies of electrons at BCP illustrates stability of the interaction. The potential energy of the electrons, G(r), expresses the pressure exerted on the electrons at the BCP by the other electrons. The kinetic energy, V(r), reflects the pressure exerted by the electrons at the BCP on the other electrons[36]. The energies in Table 3 have been calculated according to the formulas in Espinosa *et al.*[37]. The total energy, H(r) = V(r) + G(r), shows the balance between these two energies. Since the energy values in Table 3 are comparable for all the hydrogen bonds responsible for linking of the $C_8H_{16}N_4O_2$ molecules, information on stability of these hydrogen bonds can be found in other parameters as ellipticity, ε, and deviation of the hydrogen bond from linear-

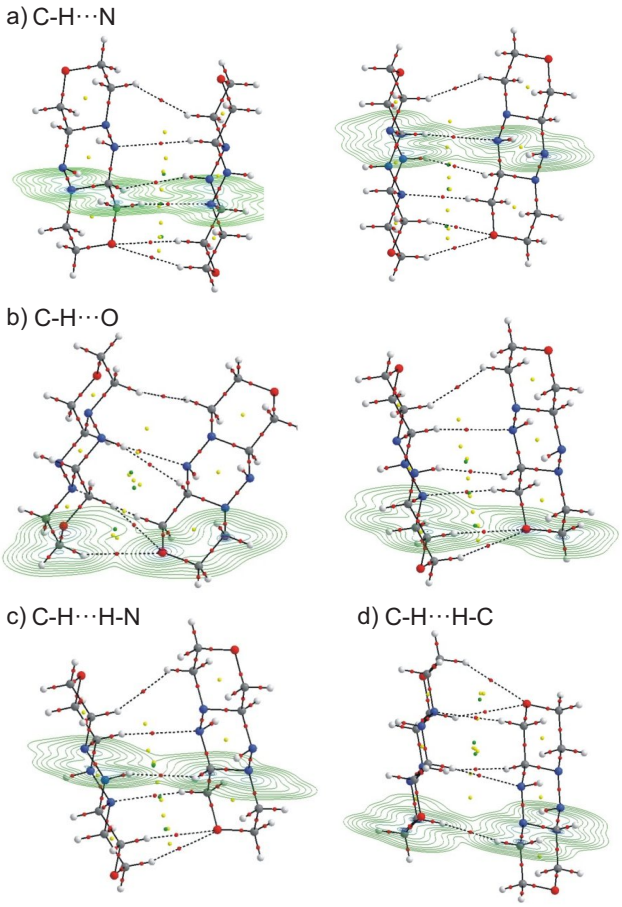

Fig. 6 Contours of the electron densities for a) C–H···N, b) C–H···O, c) C–H···H–N and d) C–H···H–C hydrogen bonds.

ity, *d*. According to Table 3 both dihydrogen bonds and the C4–H4B···O1 hydrogen bond are unstable because of high ellipticity and deviation from linearity. Nevertheless, as the structures obtained in the optimization of the dimer linked by weak hydrogen bonds show, despite high values of ε and *d* some of these interactions can be still preserved because of the close location to the quite strong C–H···N type hydrogen bonds (see below).

In the context of very weak interactions in the solid state a typical question arises: are these interactions responsible for packing of the molecules in crystal or may be the packing forces are a result of the existence of these weak interactions? To answer this question the structural motif of **1**, along with the interactions obtained from AIM theory, has been compared with the structures optimized using DFT method at different level of theory. Comparison of the crystal structure of **1** with theoretical ones is shown in Fig. 7. It is characteristic that the C–H···N type HBs – C1–H1A···O1 HB in dimer and N2–HN2···H3–C3 – are persistent in all the structures (marked with blue color in Fig. 7). Optimization at B3LYP/6-31G** level destroys C2–H2A···H2B–C2 dihydrogen bond and the protons participating in this dihydrogen bond become to be engaged in C2–H2A···N1 and C2–H2B···O1 hydrogen bonds. Comparison of the experimental and calculated hydrogen bonds can be found in Table 4. The three center hydrogen bonds linked to O1 are elongated to 3.104 and 3.014 Å. Optimization at B3LYP/6-311++G** level removes also C4–H4B···O1 hydrogen bond which in solid state is characterized by high ellipticity and nonlinearity. Comparing the X-ray and optimized structures it can be concluded that the main interactions responsible for linking the $C_8H_{16}N_4O_2$ molecules in **1** are the C–H···N type hydrogen bonds additionally stabilized by the N2–HN2···H3–C3 dihydrogen bonds. Another argument that the packing of $C_8H_{16}N_4O_2$ molecules in crystal does not change significantly the interactions in the crystal of **1** are volumes of molecular dimers in the solid state compared with the optimized dimers. These formed in the solid state are equal of 97.6% of the optimized dimer volume what suggests that the main molecular interactions in crystal are not a result of packing but the packing of the molecules in crystal results from very weak interactions.

When the $C_8H_{16}N_4O_2$ molecules are linked by water the set of hydrogen bonds is completely different comparing to **1**. As the water OH group is a very strong proton donor, the strong O1w–H1w···N2 hydrogen bond determinates the packing of the molecules. The BCP at the bond path linking water proton with the proton accepting nitrogen is characterized by high electron density value (0.0268) and low ellipticity (0.0284) typical for strong hydrogen bonds. Lone electron pairs of water accept the NH group proton of $C_8H_{16}N_4O_2$ molecules and the electron density value at the N2–HN2···O1w BCP is 0.0112. Except the NH group, the electron pair of water

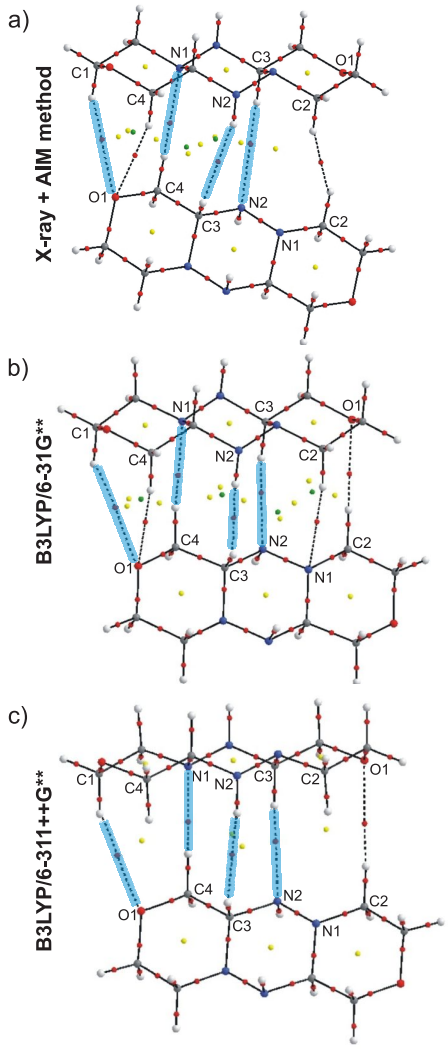

Fig. 7 Comparison of the intermolecular hydrogen bonds: X-ray structure with interactions obtained form AIM theory (a), structure optimized at B3LYP/6-31** level (b) and B3LYP/6-311++G** level (c).

Bond / method	D–H	H···A	D···A	D-H···A
C4–H4A···N1$_{exp}$	0.99	2.619	3.565	159.86
B3LYP/6–31G**	1.093	2.632	3.681	160.89
B3LYP/6–311++G**	1.090	2.670	3.704	158.24
C3–H3···N2$_{exp}$	1.00	2.956	3.898	157.42
B3LYP/6–31G**	1.101	2.619	3.708	169.66
B3LYP/6–311++G**	1.100	2.685	3.778	172.57
C1–H1A···O1$_{exp}$	0.99	2.876	3.778	151.88
B3LYP/6–31G**	1.101	3.104	4.094	150.00
B3LYP/6–311++G**	1.098	3.002	4.030	156.06
C4–H4B···O1$_{exp}$	0.99	2.806	3.729	155.36
B3LYP/6–31G**	1.102	3.011	4.027	153.24
B3LYP/6–311++G**	No bond. C···O distance of 4.688 Å.			
N2–HN2···H3–C3$_{exp}$	0.906(NH) 1.000(CH)	2.368(H···H)	3.895(N···C)	134.61(NHHC$_{tors}$)
B3LYP/6–31G**	1.030(NH) 1.106(CH)	2.194(H···H)	4.074(N···C)	-66.184(NHHC$_{tors}$)
B3LYP/6–311++G**	1.028(NH) 1.103(CH)	2.774(H···H)	4.575(N···C)	25.183(NHHC$_{tors}$)
C2–H2A···H2B–C2$_{exp}$	0.99(CH)	2.44(H···H)	4.083(C···C)	172.71(CHHC$_{tors}$)
B3LYP/6–31G**	No C2···C2 bond (distance of 4.339 Å). New bonds are formed: C2···N1 (4.162 Å) and C2···O1 (3.745 Å).			
B3LYP/6–311++G**	No C2···C2 bond (distance of 4.646 Å). New bond is formed: C2···O1 (3.980 Å).			

Table 4 Comparison of the experimental and calculated parameters of hydrogen bonds in **1**

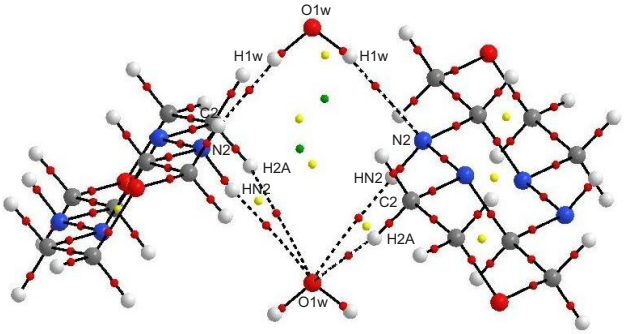

Fig. 8 The hydrogen bonds in **2** (AIM theory).

accepts also the CH proton and the C2–H2A···O1w BCP is characterized by electron density of 0.0066 and ellipticity of 0.0636. Therefore, each lone pair of water is an acceptor of two protons: one from NH and the second from CH group. The interactions of **2** are shown in Fig. 8.

The structure in which both water protons are engaged in the hydrogen bonds and the water oxygen accepts two other protons (see Fig. 9a) is very common [38] and represents 27.45% of all the structures with water listed in Cambridge Structural Database. More popular is only the water molecule with both protons engaged in a hydrogen bond and accepting one proton (38.40%, Fig. 9b). Therefore, one can easily see that the surrounding of water in **2** is not typical because of the acceptance of additional CH proton (*cf.* Fig 8). This unusual amount of the accepted protons can be explained by the shape of the oxygen lone pairs which, according to VSEPR theory, occupy two of the four tetrahedron vertices. By using Weinhold's Natural Bond Orbital (NBO) analysis [39–41] implemented in the ADF program, the oxygen lone electron pairs for the experimental X-ray structure were calculated. For the sake of brevity, only one of the obtained round-shaped oxygen lone electron pairs is depicted in Fig. 9c. Second electron pair is slightly inclined relative to the first one, and a superposition of them gives quite wide proton-attracting area. This shape of the lone pairs is responsible for the possibility of linking of two protons to each oxygen lone pair. It confirms also the statistics of the hydrogen bonds around the water molecules. Both lone pairs are located at the center of the oxygen atom what causes that the acceptance of one proton is the most popular although the shape of the lone pairs makes acceptance of many protons also possible.

Formation of the hydrate with NH bond accepted by oxygen lone pair is possible because of the conformation change of the aliphatic chains of the $C_8H_{16}N_4O_2$ molecule. In Table 5 are collected the puckering parameters calculated according to the article of Cremer *et al.* [42]. In the single optimized molecule of $C_8H_{16}N_4O_2$ the central and side rings have a chair confor-

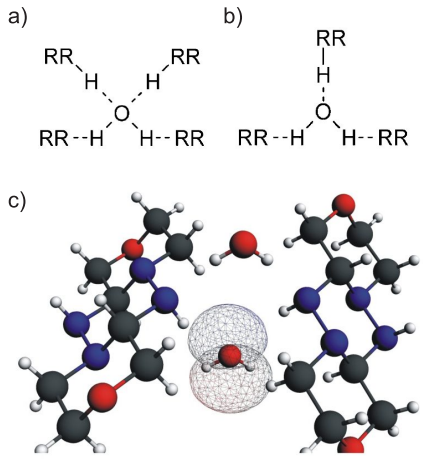

Fig. 9 a) and b) Two most common environments of water molecules[38]. c) One of the calculated lone electron pairs of water molecule.

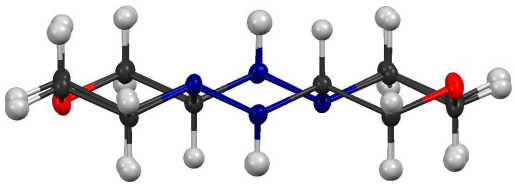

Fig. 10 An overlay of $C_8H_{16}N_4O_2$ molecules in **1** and **2**.

mation. The conformation of the side ring in **1** is markedly modified (Fig. 10). This fact coupled with the presence of weak hydrogen bonds linking the molecules may lead to thermodynamical instability that is reflected as the anomaly seen in the DSC and DTA curves during heating. The hydrated compound side ring loses its chair character. This conformation change causes that the NH group is not shielded and the proton can participate in the hydrogen bond.

2.5 Hirshfeld surface analysis

To illustrate the connectivity of molecules in **1** and **2** and to confirm the existence of weak interactions disclosed by computational methods, the Crystal Explorer program[43,44] was employed to calculate Hirshfeld surfaces of $C_8H_{16}N_4O_2$. Distance external to the surface, d_e, that measures the distance from the surface to the nearest nucleus in another molecules was mapped on the surface. The Hirshfeld surface of $C_8H_{16}N_4O_2$ in **1** is shown in Fig. 11a. The percentages of contacts that contribute to the total Hirshfeld surface area are as follows: H···H 71.6%, O···H 9.8%, H···O 7.4% and H···N 4.9%. The flat red regions marked as **a** and **b** arises from hydrogen-bond acceptors of C1–H1B···O1 and C4–H4A···N1 interactions which presence was also revealed by the single-crystal X-ray diffraction. Two C–H···O type hydrogen bonds in the *c*-axis direction possessing the same acceptor, precisely C1–H1A···O1 and C4–H4B···O1, are seen as brighter spots on the left site (**c**). As **d**, **d'**, **e** and **e'** the two dihydrogen bonds are marked: C3–H3···HN2–N2 and C2–H2B···H2A–C2, respectively. The existence of broad orange spot on the right site, **f**, turned out to be the most unexpected. As Fig. 11b shows, the colored region is a manifestation of C1–H1B···H4B–C4 interaction with H···H distance of 2.456 Å. However, the result of the analysis of this interaction with AIM theory did not confirm the existence of the dihydrogen bond as the protons are located out of the electron density path.

In the case of **2**, the interaction in which N2 atom is an acceptor of the hydrogen bond is perfectly visible on the Hirshfeld surface of $C_8H_{16}N_4O_2$, presented with d_e property (range 1.0-1.9 Å), as a wide red spot (Fig. 11c). The set of hydrogen bonds in which O1w atom of water molecule is an acceptor is shown in Fig. 11d. As one can notice, except two distinct red regions on the Hirshfeld surface of H_2O arising from N2–HN2···O1w hydrogen bonds, another two spots corresponding the C2–H2A···O1w weak hydrogen bonds manifest. Nevertheless, the most interesting seem to be marks arising from C3–H3A···O1w contacts being additional argument confirming conclusions obtained from NBO method.

3 Conclusions

The first crystallographically characterized tricyclic derivative of [1,2,4,5]-tetrazine, $C_8H_{16}N_4O_2$, showed no N–H···O and N–H···N interactions – the contacts that one would expect from the molecule structure. Instead, the interactions responsible for crystal packing that were found by single-crystal X-ray diffraction are C–H···O and C–H···N hydrogen bonds which, according to Hirshfeld surface analysis, contribute only 7.4% and 4.9%, respectively, of all contacts of $C_8H_{16}N_4O_2$ molecule. Majority of contacts, 71.6%, are H···H interactions that were investigated using AIM theory and DFT calculations. The results of the theoretical analysis helped to draw a conclusion that the packing of molecules in the crystal results from these very weak interactions.

The NH group is more active when water molecules are present in the crystal structure. N–H···Ow hydrogen bonds, along with several C–H···Ow bonds, are formed and seem to have a significant impact on thermal stability of the monohydrated analog of the compound. The unprecedented is the shape of water lone electron pairs, obtained from NBO method, that makes the acceptance of many protons possible.

	Optimized molecule		**1**		**2**	
	central ring	side ring	central ring	side ring	central ring	side ring
Q	0.5783	0.5615	1.4426	2.1729	1.4695	2.0127
Θ	180	1.0767	0	12.8936	0	58.9473
ϕ	0	163.7232	0	149.8951	0	208.7316

Table 5 Puckering parameters of $C_8H_{16}N_4O_2$ molecule: optimized, in **1** and in **2**.

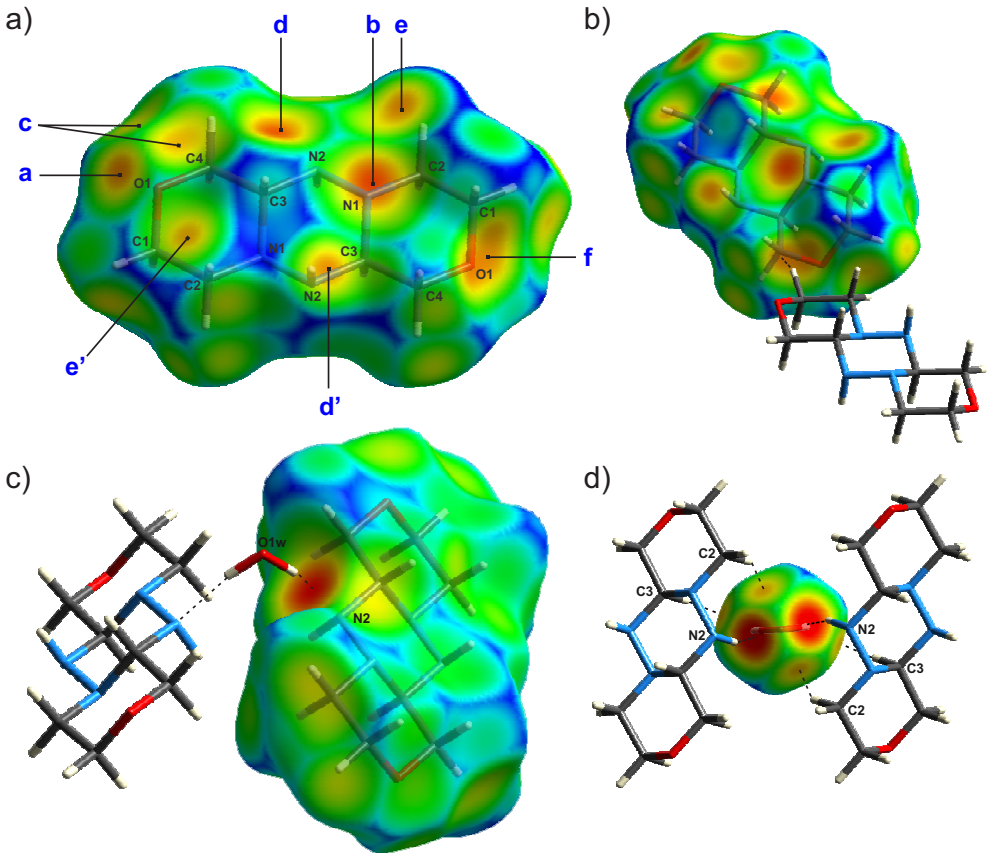

Fig. 11 a) and b) Hirshfeld surface of $C_8H_{16}N_4O_2$ in **1** with mapped distance external to the surface, d_e. Symbols **a**, **b**, **c**, **d**, **d'**, **e** and **e'** are explained in the text. c) Hirshfeld surface of $C_8H_{16}N_4O_2$ and H_2O (d) in **2** with mapped d_e. The distance external to the surface of the presented surfaces is mapped between 1.0 (red) and 1.9 Å (blue).

4 Experimental methods and calculations

Thermal properties. Simultaneous thermogravimetric analysis (TGA) and differential thermal analysis (DTA) were performed on Setaram SETSYS 16/18 instrument in the temperature range 300–880 K with a ramp rate of 2 K/min. The scans were performed in flowing nitrogen (flow rate: 1 dm^3/h). DSC curves were obtained using Perkin Elmer 8500 differential scanning calorimeter calibrated using n-heptane and indium. Hermetically sealed Al pans with the polycrystalline material were prepared in a controlled-atmosphere N_2 glovebox. The measurements were performed between 110 and 370 K.

X-ray measurements. The X-ray diffraction data for **1** and **2** were collected at 100 K on a Xcalibur diffractometer with graphite monochromated Mo Kα radiation, equipped with an Oxford Cryosystem cooling device. The crystal structures were solved by direct methods with the SHELXS97 program[45] and refined by a full-matrix least-squares method on all F^2 data. All nonhydrogen atoms were refined with anisotropic temperature factors. The C-bound H atoms were located from the molecular geometry and their isotropic temperature factors U_{iso} were assumed as 1.2 $\times$ U_{eq} of their closest heavy atoms, respectively. The H atoms of NH group and H1w atom (from water molecule in **2**) were located on difference Fourier map and refined with displacement parameters being equal to 1.2 times U_{eq} and 1.5 times U_{eq} of the attached N and O1w atoms, respectively. CrysAlis software (Oxford Diffraction Company) was used in data collection, cell refinement and data reduction processes[46]. The crystallographic data of the studies of **1** and **2** are given in Table 1. Crystallographic data for the structures reported in this paper have been deposited with the Cambridge Crystallographic Data Centre, CCDC Nos. 953930-1.

Computational details. Wave function files (.wfn) were generated using Gaussian 09 program[47] with the crystal structure of **1** and **2** used as a starting point. In the case of **1**, AIM analyses of two $C_8H_{16}N_4O_2$ molecules linked with two identical C–H$\cdots$O hydrogen bonds forming a cyclic dimer, and of two $C_8H_{16}N_4O_2$ molecules linked by weak hydrogen bonds along *c*-axis, were performed with the AIMAll program[48]. The latter arrangement was than optimized at the DFT B3LYP/6–31G** and B3LYP/6–311++G** levels of calculation by using Gaussian 09 program and AIM analysis was performed again. In the case of **2**, AIM analysis was performed of a cluster of two $C_8H_{16}N_4O_2$ molecules with two molecules of H_2O. The Natural Bond Orbital (NBO) analysis, of X-ray crystal structure of **2**, was performed with the ADF program[49,50].

5 Acknowledgements

We thank the Wroclaw Center for Networking and Supercomputing for generous computer time. The programme of the Polish Plenipotentiary in JINR Nr 61 from 11.02.2013, p.12, is acknowledged.

References

1 C. G. Overberger and B. S. Marks, *J. Am. Chem. Soc.*, 1955, **77**, 4104–4107.
2 W. R. McBride and E. M. Bens, *J. Am. Chem. Soc.*, 1959, **81**, 5546–5550.
3 C. G. Overberger, N. P. Marullo and R. G. Hiskey, *J. Am. Chem. Soc.*, 1961, **83**, 1374–1378.
4 D. M. Lemal, T. W. Rave and S. D. McGregor, *J. Am. Chem. Soc.*, 1963, **85**, 1944–1948.
5 C. L. Bumgardner, K. J. Martin and J. P. Freeman, *J. Am. Chem. Soc.*, 1963, **85**, 97–99.
6 D. M. Lemal and T. W. Rave, *J. Am. Chem. Soc.*, 1965, **87**, 393–394.
7 D. M. Lemal, C. D. Underbrink and T. W. Rave, *Tetrahedron Lett.*, 1964, **29**, 1955–1960.
8 C. Darwich, M. Elkhatib, G. Steinhauser and H. Delalu, *Kinet. Catal.*, 2009, **50**, 103–110.
9 Z. Huang, J. Zhou and J. F. Hartwig, *J. Am. Chem. Soc.*, 2010, **132**, 11458–11460.
10 K. Gholivand, Z. Hosseini, S. Farshadian and H. Naderi-Manesh, *Eur. J. Med. Chem.*, 2010, **45**, 5130–5139.
11 M. C. Etter, *J. Phys. Chem.*, 1991, **95**, 4610–4618.
12 A. I. Kitaigorodskii, *Organic Chemical Crystallography*, Consultants Bureau, New York, 1961.
13 R. F. W. Bader, *Atoms in Molecules: A Quantum Theory*, Oxford University Press, Oxford, 1990.
14 A. B. C. F. Matta, R. J. Boyd, *The Quantum Theory of Atoms in Molecules: From Solid State to DNA and Drug Design*, Wiley-VCH, 2007.
15 P. L. Popelier, *Atoms in Molecules: An Introduction*, Prentice Hall, 1st edn., 2000.
16 Y. Mo, *J. Phys. Chem. A*, 2012, **116**, 5240–5246.
17 I. Majerz, *J. Phys. Chem. A*, 2012, **116**, 7992–8000.
18 I. Majerz, *Org. Biomol. Chem.*, 2011, **9**, 1466–1473.
19 I. Majerz, *Mol. Phys.*, 2007, **105**, 2305–2314.
20 P. L. A. Popelier and R. F. W. Bader, *J. Phys. Chem.*, 1994, **98**, 4473–4481.
21 U. Koch and P. L. A. Popelier, *J. Phys. Chem.*, 1995, **99**, 9747–9754.
22 P. L. A. Popelier, *J. Phys. Chem. A*, 1998, **102**, 1873–1878.
23 W. T. Klooster, T. F. Koetzle, P. E. M. Siegbahn, T. B. Richardson and R. H. Crabtree, *J. Am. Chem. Soc.*, 1999, **121**, 6337–6343.
24 P. C. Singh and G. N. Patwari, *Chem. Phys. Lett.*, 2006, **419**, 265–268.
25 P. Lipkowski, S. J. Grabowski, T. L. Robinson and J. Leszczynski, *J. Phys. Chem. A*, 2004, **108**, 10865–10872.
26 E. S. Shubina, N. V. Belkova, A. N. Krylov, E. V. Vorontsov, L. M. Epstein, D. G. Gusev, M. Niedermann and H. Berke, *J. Am. Chem. Soc.*, 1996, **118**, 1105–1112.
27 T. B. Richardson, S. de Gala, R. H. Crabtree and P. E. M. Siegbahn, *J. Am. Chem. Soc.*, 1995, **117**, 12875–12876.
28 C. F. Matta, L. Huang and L. Massa, *J. Phys. Chem. A*, 2011, **115**, 12451–12458.
29 C. F. Matta, N. Castillo and R. J. Boyd, *J. Phys. Chem. B*, 2006, **110**, 563–578.
30 C. F. Matta, N. Castillo and R. J. Boyd, *J. Phys. Chem. A*, 2005, **109**, 3669–2681.
31 R. J. Boyd and S. C. Choi, *Chem. Phys. Lett.*, 1985, **120**, 80–85.
32 R. J. Boyd and S. C. Choi, *Chem. Phys. Lett.*, 1986, **129**, 62–65.
33 O. Knop, K. N. Rankin and R. J. Boyd, *J. Phys. Chem. A*, 2003, **107**, 272–284.

34 O. Knop, R. J. Boyd and S. C. Choi, *J. Am. Chem. Soc.*, 1988, **110**, 7299–7301.

35 N. Castillo, K. N. Robertson, S. C. Choi, R. J. Boyd and O. Knop, *J. Comput. Chem.*, 2007, **29**, 367–379.

36 E. Espinosa, I. Alkorta, J. Elguero and E. J. Molins, *J. Chem. Phys.*, 2002, **117**, 5529–5542.

37 E. Espinosa, I. Alkorta, I. Rozas, J. Elguero and E. J. Molins, *Chem. Phys. Lett.*, 2002, **336**, 457–461.

38 A. L. Gillon, N. Feeder, R. J. Davey and R. Storey, *Cryst. Growth Des.*, 2003, **3**, 663–673.

39 P.-O. Löwdin, *Phys. Rev.*, 1955, **97**, 1474–1489.

40 F. Weinhold and C. R. Landis, *Chem. Educ. Res. Pract. Eur.*, 2001, **2**, 91–104.

41 G. N. Lewis, *J. Am. Chem. Soc.*, 1916, **38**, 762–785.

42 D. Cremer and J. A. Pople, *J. Am. Chem. Soc.*, 1975, **97**, 1354–1358.

43 S. K. Wolff, D. J. Grimwood, J. J. McKinnon, M. J. Turner, D. Jayatilaka and M. A. Spackman, *CrystalExplorer (Version 3.0)*, 2012.

44 J. J. McKinnon, M. A. Spackman and A. S. Mitchell, *Acta Crystallogr., Sect. B: Struct. Sci.*, 2004, **60**, 627–668.

45 G. M. Sheldrick, *Acta Crystallogr., Sect. A: Found. Crystallogr.*, 2008, **A64**, 112–122.

46 Oxford Diffraction Poland, *CrysAlis RED*, 1995-2003.

47 M. Frisch, G. W. Trucks, H. B. Schlegel, G. E. Scuseria, M. A. Robb, J. R. Cheeseman, G. Scalmani, V. Barone, B. Mennucci, G. A. Petersson, H. Nakatsuji, M. Caricato, X. Li, H. P. Hratchian, A. F. Izmaylov, J. Bloino, G. Zheng, J. L. Sonnenberg, M. Hada, M. Ehara, K. Toyota, R. Fukuda, J. Hasegawa, M. Ishida, T. Nakajima, Y. Honda, O. Kitao, H. Nakai, T. Vreven, J. A. Montgomery, Jr., J. E. Peralta, F. Ogliaro, M. Bearpark, J. J. Heyd, E. Brothers, K. N. Kudin, V. N. Staroverov, R. Kobayashi, J. Normand, K. Raghavachari, A. Rendell, J. C. Burant, S. S. Iyengar, J. Tomasi, M. Cossi, N. Rega, J. M. Millam, M. Klene, J. E. Knox, J. B. Cross, V. Bakken, C. Adamo, J. Jaramillo, R. Gomperts, R. E. Stratmann, O. Yazyev, A. J. Austin, R. Cammi, C. Pomelli, J. W. Ochterski, R. L. Martin, K. Morokuma, V. G. Zakrzewski, G. A. Voth, P. Salvador, J. J. Dannenberg, S. Dapprich, A. D. Daniels, . Farkas, J. B. Foresman, J. V. Ortiz, J. Cioslowski and D. J. Fox, *Gaussian 09 Revision C.01*.

48 T. A. Keith, *AIMAll (Version 13.02.26)*, TK Gristmill Software, Overland Park KS, USA, 2012.

49 G. te Velde, F. M. Bickelhaupt, E. J. Baerends, C. F. Guerra, S. J. A. van Gisbergen, J. G. Snijders and T. Ziegler, *J. Comput. Chem.*, 2001, **22**, 931–967.

50 C. F. Guerra, J. G. Snijders, G. te Velde and E. J. Baerends, *Theor. Chem. Acc.*, 1998, **99**, 391–403.

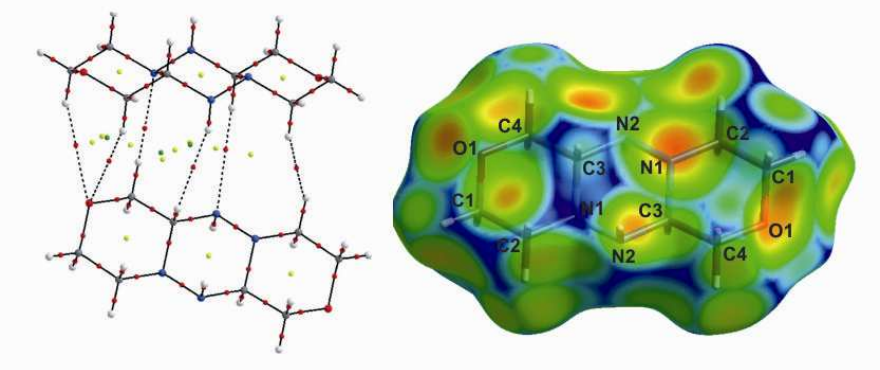

Experimental (single-crystal X-ray diffraction) and theoretical (AIM, DFT, NBO, Hirshfeld surface) studies have been performed to elucidate intermolecular interactions of the anhydrous $C_8H_{16}N_4O_2$ and its monohydrated analog.